Machine-Learning Defined Precision tDCS for Improving Cognitive Function

Alejandro Albizu^{1,2}, Aprinda Indahlastari^{1,5}, Ziqian Huang^{1,4}, Jori Waner^{1,5}, Skylar E. Stolte^{1,3}, Ruogu Fang^{1,3,4,†}, and Adam J. Woods^{1,2,5,†}

- ¹ Center for Cognitive Aging and Memory, McKnight Brain Institute, University of Florida, Gainesville, USA
- ² Department of Neuroscience, College of Medicine, University of Florida, Gainesville, USA
- ³ J. Crayton Pruitt Family Department of Biomedical Engineering, Herbert Wertheim College of Engineering, University of Florida, Gainesville, USA
- ⁴ Department of Electrical and Computer Engineering, Herbert Wertheim College of Engineering, University of Florida. Gainesville. USA
- ⁵ Department of Clinical and Health Psychology, College of Public Health and Health Professions, University of Florida, Gainesville, USA
- [†] Co-corresponding authors

Abstract

Background

Transcranial direct current stimulation (tDCS) paired with cognitive training (CT) is widely investigated as a therapeutic tool to enhance cognitive function in older adults with and without neurodegenerative disease. Prior research demonstrates that the level of benefit from tDCS paired with CT varies from person to person, likely due to individual differences in neuroanatomical structure.

Objective

The current study aims to develop a method to objectively optimize and personalize current dosage to maximize the functional gains of non-invasive brain stimulation.

Methods

A support vector machine (SVM) model was trained to predict treatment response based on computational models of current density in a sample dataset (n = 14). Feature weights of the deployed SVM were used in a weighted Gaussian Mixture Model (GMM) to maximize the likelihood of converting tDCS non-responders to responders by finding the most optimum electrode montage and applied current intensity (optimized models).

Results

Current distributions optimized by the proposed SVM-GMM model demonstrated 93% voxel-wise coherence within target brain regions between the originally non-responders and responders. The optimized current distribution in original non-responders was 3.38 standard deviations closer to the current dose of responders compared to the preoptimized models. Optimized models also achieved an average treatment response likelihood and normalized mutual information of 99.993% and 91.21%, respectively. Following tDCS dose optimization, the SVM model successfully predicted all tDCS nonresponders with optimized doses as responders.

Conclusions

The results of this study serve as a foundation for a custom dose optimization strategy towards precision medicine in tDCS to improve outcomes in cognitive decline remediation for older adults.

Keywords

tES, Aging, Machine-learning, Finite element model, Gaussian Mixture Model, Precision Medicine

Introduction

Previous longitudinal and cross-sectional clinical studies in aging populations converge on the idea that subtle declines in working memory are a natural part of the aging process [1-5]. Effective interventions to prevent working memory decline and enhance brain function in older adults remain elusive. Such interventions will be necessary to reduce the projected prevalence of cognitive impairment and Alzheimer's disease over the coming decades [6]. Transcranial direct current stimulation (tDCS), a form of weak non-invasive electrical brain stimulation, has demonstrated moderate to large effect sizes to remediate cognitive aging in the healthy older adult population [7,8]. The putative mechanism of tDCS is based on the alteration of resting membrane potentials (i.e., modulate or attenuate) [9]. Thus, tDCS can facilitate or impede endogenous presynaptic potentials within the local field of stimulation, akin to either a long-term potentiation or depression [10-18]. Indeed, recent research suggests that tDCS-modulated neuroplasticity paired with cognitive training (CT) can enhance outcomes in older adults [19–22]. However, the level of benefit from tDCS paired with cognitive training varies from person to person, likely due to individual differences in neuroanatomical structure. The finite element method (FEM) can be used to account for individual differences in neuroanatomical structure through MRI-derived estimation of the tDCS electric field [23-31]. Individualized tDCS modeling has been shown to predict functional connectivity [32], motor-evoked potentials [33], and cortical blood oxygenation [34,35]. Recent research has also shown that machine learning has the potential to identify factors critical in optimizing stimulation outcomes in each person by accounting for these individual differences [36-39]. The current study employs state-of-the-art MRI-derived computational modeling (i.e., FEM) and machine learning to determine the tDCS parameters that maximize in-silico treatment response likelihood.

To date, all prior trials of tDCS have applied a fixed dosing strategy (e.g., 2 mA for 20 min with electrodes at F3/F4 in the 10-20 system) for all recipients. Our previous study [36], demonstrated that electrical current intensity and direction within the brain were strongly associated with treatment response. However, prior research demonstrates that individual variability in anatomical structures (e.g., brain atrophy, skull thickness, etc.), especially in older adults, generates significant variability in the spread and intensity of directed electrical current delivered to the brain [26,29,30,40]. Considering inherent dosing variability across individuals, optimization algorithms can be applied to patient-specific, MRI-derived computational models of electric current. Such an application has potential utility in determining tDCS parameters that optimize each individual's electric field within the brain, maximizing the statistical likelihood of treatment response. We hypothesized that individual differences in neuroanatomical structure contribute to the variability seen in the amount of tDCS current reaching the brain tissue, which may subsequently alter individual treatment response. Given this, there have been some studies that have attempted an optimized electric-field approach, and these studies have shown promising results [41–44]. However, previous tDCS optimization techniques have utilized numerical approaches to search the parameter space, such as linear programming [41-44]. Although numerical techniques have been successful for convex problems, they may converge on suboptimal solutions when dealing with non-convex problems, which are common in real-world optimization due to the presence of multiple local optima. Additionally, previous tDCS optimization studies also required an a priori determination of brain regions and electric field characteristics to target, such as maximizing current intensity or focality. Instead, we propose an alternative exhaustive search approach that is purely data driven, leveraging SVM and GMM to account for individual anatomical differences. The SVM model provides the essential dosing characteristics for treatment response (i.e., current distribution, intensity, and direction) while the exhaustive GMM

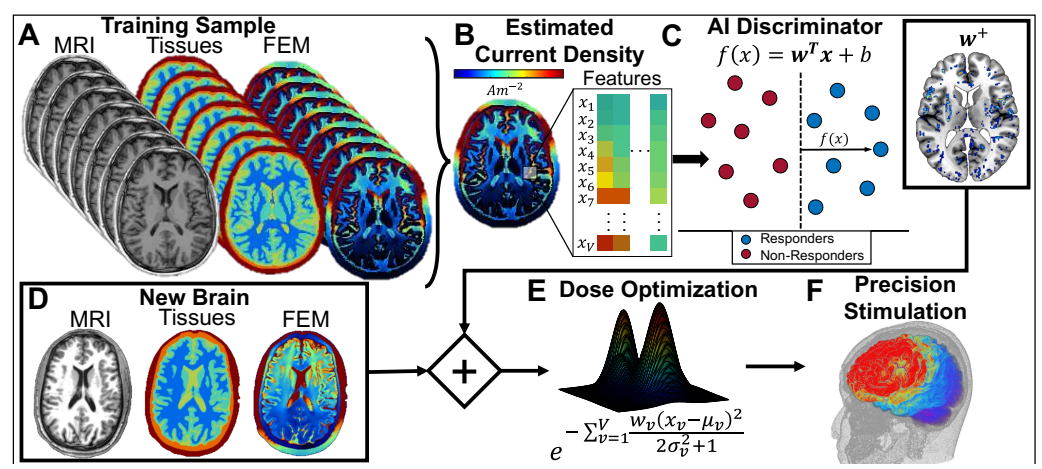


Figure 1. A schematic diagram of the proposed SVM-GMM tDCS precision dosing pipeline: **A)** a dataset of structural MRI-images is used to train the machine learning discriminator. **B)** Specifically, individual computational models (Am⁻²) with colors representing estimated current density within each voxel of the head are used as features. **C)** These data are submitted to a machine learning discriminator to predict treatment response and output feature weights representing the predictive power of each voxel, **D)** Similar computational models of current density can be computed from MRI-images from a novel, treatment naïve brain. **E)** Computational models of treatment naïve computational models can then be submitted to a weighted, Gaussian mixture model to optimize tDCS dosing parameters. **F)** The electrode montage and injected current intensity that maximize the likelihood of treatment response are used as precision doses.

parameter search ensures the best possible parameters to achieve treatment response. This SVM-GMM approach will significantly increase the statistical likelihood of treatment response and precisely match the electrical current profile of treatment responders.

Methods

A T1-weighted Magnetic Resonance Imaging (MRI) dataset of 14 healthy older adults (mean (sd) age = 73.57 (7.84), mean (sd) MoCA = 27.85 (1.79), 7F:7M) was utilized to create individualized FEM. Details of the clinical trial dataset (NCT02137122; [19]) and machine learning protocol [36] have been previously reported. Responder and nonresponder labels were derived via a median split of working memory improvements following tDCS [36]. The current density distribution in each brain was computed using an open-source FEM software ROAST v3.0 [24]. Individual head volumes were segmented into six tissue types: white matter, gray matter, cerebrospinal fluid, bone, skin, and **HEADRECO** [25]—provided intracranial bν SimNIBS (https://simnibs.github.io/simnibs/build/html/index.html). Individual tissue types were assigned conductivity values in ROAST [24]. Segmentation quality was visually inspected by overlaying segmented masks onto their respective T1-weighted images. Pad electrodes (5 x 7 cm²) were simulated as anodes at all 71 locations within the standard 10-10 EEG system [45,46]. Each anode electrode was paired with a fixed, "reference" cathode at I₂ and electric field models were generated per pair (i.e., two electrodes per model) yielding 71 unique electric field distributions to serve as the lead field for each head model. These lead fields can then be linearly combined to yield a standard montage (e.g., F4 Lead Field - F3 Lead Field = F3 Cathode/F4 Anode, see Dmochowski et al. 2011 for details [47]). This approach allows the estimation of any electrode montage without the need to exhaustively compute each model [47] Click or tap here to enter text.. Generated electric fields (E, in the unit of [Vm⁻¹]) were then converted into current densities (J, in the unit of [A m⁻²]) based on the conductivity of the tissues.

A support vector machine (SVM) learning algorithm was used in our previous study to classify responders and non-responders based on the computed current density distribution per individual (in this case, F3/F4 at 2mA). In this study, the model produced an overall prediction accuracy of 86.43% (details for data processing and SVM model generation can be found in our previously published study [36]). In sum, LIBSVM [48] was used to optimize the objective function:

$$\min_{w,b} \frac{1}{2} w^T w + C \sum_{n=1}^{N} \max (1 - y_n (w^T x_n + b), 0)^2$$

where $C \ge 0$ is a penalty parameter on the training error. y_n and x_n are the ground truth label and feature vector for the n^{th} of N total observations, respectively. The SVM model was trained to optimize parameters w and b, which represent the weight and bias respectively. Optimized weights in the SVM model were used in a modified, weighted Gaussian mixture model (GMM) to generate a precision model that accounts for interpersonal variation based on the current distribution of responders.

The empirical responder mean, empirical responder variance, and SVM feature weights were used to estimate each Gaussian model. The likelihood (1) of a new subject belonging to the responders' current distribution (i.e., response likelihood) was calculated using:

$$\ell(x \mid w, \mu, \sigma) = e^{-\sum_{v=1}^{V} \frac{w_v(x_v - \mu_v)^2}{2\sigma_v^2 + 1}}$$

where w_v is the SVM weight (s.t., $\sum w = 1$), μ_v is the empirical responder mean, and σ_v^2 is the empirical responder variance for the v^{th} of V features. The likelihood estimate was used as the objective function to optimize tDCS parameters (i.e., electrode placement and injected current intensity; see Figure 1) in each current density volume.

Normalized mutual information, feature-wise regression, and feature-wise dot product were used as metrics to evaluate the performance of optimization. To that end, normalized mutual information was defined as:

$$I(x,y) = \max\left(\frac{H(x) + H(y) - H(x,y)}{\sqrt{H(x) \times H(y)}}, 0\right)$$

 $I(x,y) = \max{(\frac{H(x)+H(y)-H(x,y)}{\sqrt{H(x)\times H(y)}},0)}$ where $H(i) = -p(i)\cdot \log_2 p(i)$ represents the entropy of a given distribution. Principal component analysis (PCA) was also utilized to project the expansive feature space and Gaussian model into two dimensions (i.e., the first two principal components). Electrode positions were optimized from 71x70=4,970 potential electrode pairs considering the electrical current direction (71 locations from the 10-10 system). The injected current intensity was optimized between 0.1 through 4.0 mA in 0.1 mA increments for a total of 40 possible input current levels. The overall tDCS optimization space included 198,800 potential tDCS doses per person. An exhaustive search of the parameter space was carried out in parallel on 7 NVIDIA A100 80GB GPUs with NVIDIA's RAPIDS AI package (https://rapids.ai) to ensure the global maximum response likelihood. After the optimization process, current density volumes of optimized doses within the non-responder group were passed back through the original SVM model to predict treatment responders or nonresponders.

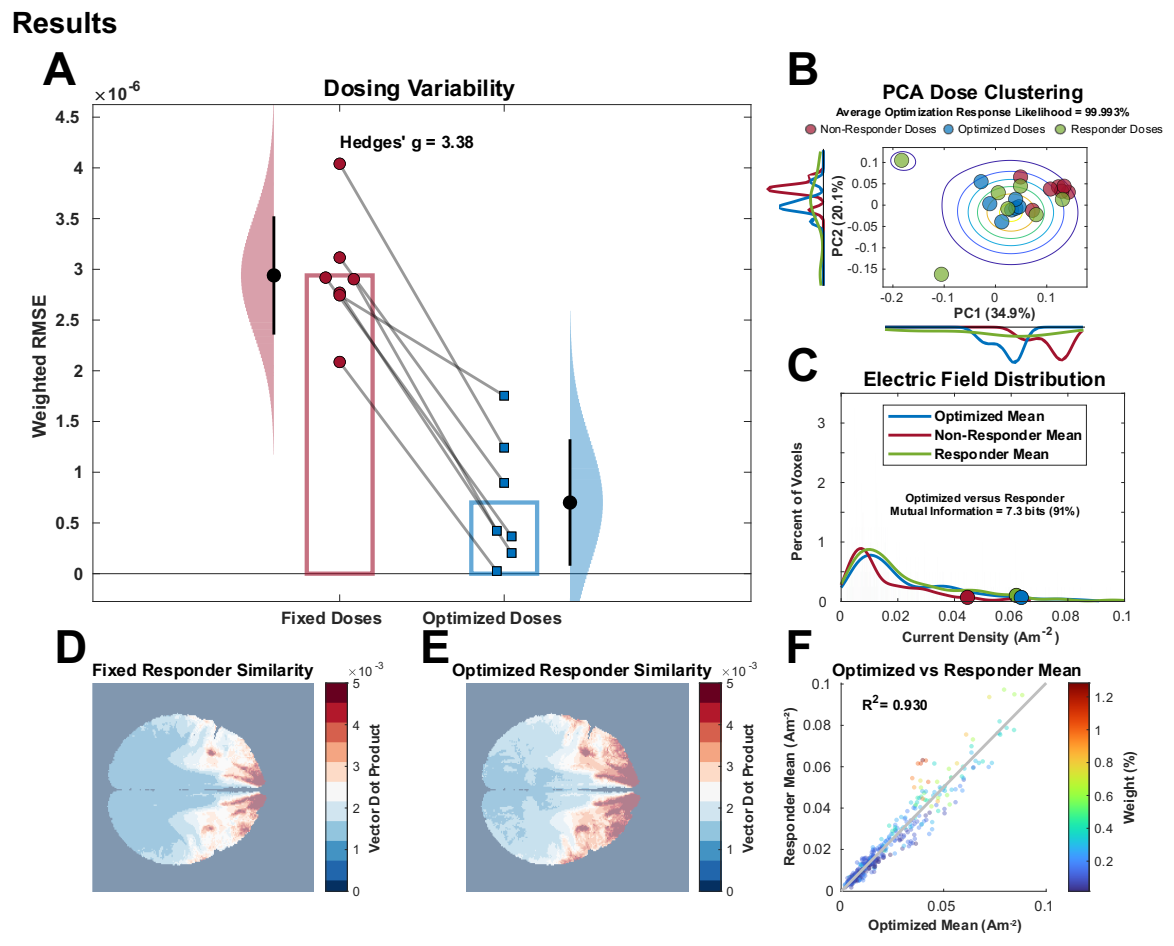


Figure 2. Conventional fixed dosing compared to optimized dosing. **A)** Dosing variability represented as root mean squared error (RMSE) in average current density reaching the brain by fixed versus optimized doses respectively compared to the average responder current density reaching the brain. Black dots represent the mean. Error bars represent ±1 SD from the mean. Histograms represent the normal distribution of the sample. **B)** Response likelihood of non-responder (red) optimized (blue), and responder (green) models. Contour lines represent a 3D Gaussian distribution of the first and second principal components (*i.e.*, PC1 and PC2) for responders. Histograms represent the smoothed distribution of PC1 and PC2 for estimated current density. **C)** Estimated current density reaching the brain for responder (green), non-responder (red), and optimized (blue) dosing. Dots represent the 95th percentile of each distribution. **D)** 3D dot product of the mean current density vector for the fixed versus responder mean. **E)** 3D dot product of current density vectors for average optimized dose versus average responder dose. **F)** Scatter plot of the voxel-wise mean current density of optimized doses versus the voxel-wise mean current density of tDCS responders.

As previously reported, computational models of current intensity and direction predicted treatment response with over 86% accuracy [36]. Following GMM optimization, non-responders were 3.38 pooled standard deviations closer to the responder mean compared to pre-optimization fixed dosing of non-responders (cf. Figure 2A, F[1,12] = 48.12, p < 0.001, g = 3.38). GMM dose optimization also achieved an average response likelihood of 99.993% (cf. Figure 2B) and shared 91.21% (7.26 bits) of normalized mutual information with the mean current distribution for responders (cf. Figure 2C). Regression of the mean optimized current density vector demonstrated strong featurewise coherence (cf. Figure 2F, $R^2 = 0.930, p < 0.001$) and elevated the average featurewise dot product with the current density vector of responders (cf. current density similarity to responders) by 40.8% compared to the conventional non-responder fixed doses (cf. Figure 2D & 2E). To assess optimization generalizability, five independent

older adult E-fields were optimized using GMM. These out-of-sample data achieved an average response likelihood of 98.8% after optimization. All were classified as responders by the original SVM. Thus, the optimized electrical distribtion of the original non-responders were 100% converted to treatment responders *in-silico* via the proposed precision dosing approach.

Discussion

At present, the optimal stimulation target areas and anatomical substrates of tDCS remain unknown. Given the large individual variability in head anatomy, the conventional a priori electrode placement and injected current approach of tDCS is unlikely to optimally distribute current for maximal treatment response [28,49,50]. The current study is a follow-up analysis to our previous treatment response prediction study [36] and, to the best of our knowledge, the first to utilize MRI-derived computational models, machine learning, and dose optimization to maximize the likelihood of treatment response at an individual level based on previously analyzed responders' group of working memory performance. Our prior study demonstrated that features of MRI-derived electric fields can successfully predict working memory improvements with over 86% accuracy. Given this information, the current study used GMM optimization to significantly improve the electric field profile and match tDCS responders compared to a conventional fixed dosing strategy by customizing tDCS parameters for each individual that maximize the Gaussian likelihood of treatment response *in silico*.

Overall, leveraging these precision dosing techniques provides a tool to potentially address necessary questions for enhancing the efficacy of tDCS paired with CT for remediating cognitive decline in older adults. Therefore, the present study provides critical information that can further improve existing prediction of tES current characteristics in older adults and a platform towards current dose customization for future tES applications in older adults. We acknowledge that our proposed approach involves relatively high computational resources due to the exhaustive search of tDCS parameters for each individual patient. This may limit its practical use in acute clinical settings requiring rapid treatment response. Therefore, future studies are needed to explore other relevant optimization procedures that are more efficient algorithms to reduce the computation time while maintaining the precision of the results. Additionally, while the models presented in this study show promise in silico, it is important to validate the precision doses in vivo through clinical trials. Furthermore, the analyses were performed on a small clinical trial dataset (NCT02137122), and thus, replication of these results with a larger, more heterogeneous sample is recommended to establish the generalizability of our findings. Conducting clinical trials to assess the potential of these precision dosing strategies is crucial for advancing the field and evaluating the efficacy and safety of individualized tDCS treatments.

In conclusion, the presented results demonstrate a novel, dose optimization paradigm for non-invasive electrical stimulation. Machine learning combined with patient-specific MRI-based models of the head is used to determine the electrode positions and current intensities to maximize the likelihood of treatment response by optimizing the induced electric field distribution. It was shown, at least computationally, that the optimal stimulation parameters improved response likelihood prediction, and elevated current intensity within targeted brain regions, and closely resembled the current distributions observed in treatment responders. Therefore, the current study demonstrates a precision dosing model of non-invasive brain stimulation to potentially improve treatment outcomes. While the current use case relates to remediating age-related decline in cognition, the potential use cases for this approach may far exceed this example. The next steps will

involve directly assessing whether these paradigms, when applied in clinical trials, can improve treatment response beyond conventional dosing methods.

Acknowledgments

This work was supported by the National Institutes of Health/National Institute on Aging (RF1AG071469, R01AG054077, K01AG050707), the National Science Foundation (1842473,1908299), the University of Florida McKnight Brain Institute and the McKnight Brain Research Foundation. The content is solely the responsibility of the authors and does not necessarily represent the official views of the National Institutes of Health and the National Science Foundation.

We gratefully acknowledge the support of NVIDIA AI Tech Center (NVAITC) to this research project, especially the great support with GPU and MPI technology from Oded Green (NVAITC), Jingchao Zhang (NVAITC), and Kaleb Smith (NVAITC).

REFERENCES

- [1] Blazer D, Yaffe K, Liverman C. Characterizing and assessing cognitive aging. Cognitive Aging: Progress in Understanding and Opportunities for Action 2015:31–74.
- [2] Blazer DG, Yaffe K, Liverman CT. Cognitive aging: Progress in understanding and opportunities for action. 2015. https://doi.org/10.17226/21693.
- [3] Salthouse TA. Trajectories of normal cognitive aging. Psychology and Aging 2019. https://doi.org/10.1037/pag0000288.
- [4] Cohen RA, Marsiske MM, Smith GE. Neuropsychology of aging. Handbook of Clinical Neurology, vol. 167, Elsevier B.V.; 2019, p. 149–80. https://doi.org/10.1016/B978-0-12-804766-8.00010-8.
- [5] Salthouse TA. When does age-related cognitive decline begin? Neurobiology of Aging 2009;30:507–14. https://doi.org/10.1016/j.neurobiolaging.2008.09.023.
- [6] Matthews KA, Xu W, Gaglioti AH, Holt JB, Croft JB, Mack D, et al. Racial and ethnic estimates of Alzheimer's disease and related dementias in the United States (2015–2060) in adults aged ≥65 years. Alzheimer's and Dementia 2019;15:17–24. https://doi.org/10.1016/j.jalz.2018.06.3063.
- [7] Indahlastari A, Hardcastle C, Albizu A, Alvarez-Alvarado S, Boutzoukas EM, Evangelista ND, et al. A Systematic Review and Meta-Analysis of Transcranial Direct Current Stimulation to Remediate Age-Related Cognitive Decline in Healthy Older Adults. Neuropsychiatric Disease and Treatment 2021;Volume 17:971–90. https://doi.org/10.2147/NDT.S259499.
- [8] Bennett IJ, Madden DJ. Disconnected aging: Cerebral white matter integrity and age-related differences in cognition. Neuroscience 2014;276:187–205. https://doi.org/10.1016/j.neuroscience.2013.11.026.
- [9] Albizu A, Indahlastari A, Woods AJ. Non-invasive Brain Stimulation. Encyclopedia of Gerontology and Population Aging, Springer International Publishing; 2019, p. 1–8. https://doi.org/10.1007/978-3-319-69892-2_682-1.
- [10] Kronberg G, Rahman A, Sharma M, Bikson M, Parra LC. Direct current stimulation boosts hebbian plasticity in vitro. Brain Stimulation 2020. https://doi.org/10.1016/j.brs.2019.10.014.
- [11] Jackson MP, Rahman A, Lafon B, Kronberg G, Ling D, Parra LC, et al. Animal models of transcranial direct current stimulation: Methods and mechanisms. Clinical Neurophysiology 2016. https://doi.org/10.1016/j.clinph.2016.08.016.
- [12] Kronberg G, Bridi M, Abel T, Bikson M, Parra LC. Direct Current Stimulation Modulates LTP and LTD: Activity Dependence and Dendritic Effects. Brain Stimulation 2017. https://doi.org/10.1016/j.brs.2016.10.001.
- [13] Ranieri F, Podda Riccardi E, Frisullo G, Dileone M, Profice P, et al. Modulation of LTP at rat hippocampal CA3-CA1 synapses by direct current stimulation. Journal of Neurophysiology 2012. https://doi.org/10.1152/jn.00319.2011.
- [14] Podda MV, Cocco S, Mastrodonato A, Fusco S, Leone L, Barbati SA, et al. Anodal transcranial direct current stimulation boosts synaptic plasticity and memory in mice via epigenetic regulation of Bdnf expression. Scientific Reports 2016. https://doi.org/10.1038/srep22180.

- [15] Monai H, Ohkura M, Tanaka M, Oe Y, Konno A, Hirai H, et al. Calcium imaging reveals glial involvement in transcranial direct current stimulation-induced plasticity in mouse brain. Nature Communications 2016;7:1–10. https://doi.org/10.1038/ncomms11100.
- [16] Fritsch B, Reis J, Martinowich K, Schambra HM, Ji Y, Cohen LG, et al. Direct current stimulation promotes BDNF-dependent synaptic plasticity: Potential implications for motor learning. Neuron 2010;66:198–204. https://doi.org/10.1016/j.neuron.2010.03.035.
- [17] Márquez-Ruiz J, Leal-Campanario R, Sańchez-Campusano R, Molaee-Ardekani B, Wendling F, Miranda PC, et al. Transcranial direct-current stimulation modulates synaptic mechanisms involved in associative learning in behaving rabbits. Proceedings of the National Academy of Sciences of the United States of America 2012. https://doi.org/10.1073/pnas.1121147109.
- [18] Lafon B, Rahman A, Bikson M, Parra LC. Direct Current Stimulation Alters Neuronal Input/Output Function. Brain Stimulation 2017;10:36–45. https://doi.org/10.1016/j.brs.2016.08.014.
- [19] Nissim NR, O'Shea A, Indahlastari A, Kraft JN, von Mering O, Aksu S, et al. Effects of Transcranial Direct Current Stimulation Paired With Cognitive Training on Functional Connectivity of the Working Memory Network in Older Adults. Frontiers in Aging Neuroscience 2019;11:340. https://doi.org/10.3389/fnagi.2019.00340.
- [20] Gomes-Osman J, Indahlastari A, Fried PJ, Cabral DLF, Rice J, Nissim NR, et al. Non-invasive Brain Stimulation: Probing Intracortical Circuits and Improving Cognition in the Aging Brain. Frontiers in Aging Neuroscience 2018;10. https://doi.org/10.3389/fnagi.2018.00177.
- [21] Cruz Gonzalez P, Fong KNK, Chung RCK, Ting KH, Law LLF, Brown T. Can transcranial direct-current stimulation alone or combined with cognitive training be used as a clinical intervention to improve cognitive functioning in persons with mild cognitive impairment and dementia? A systematic review and meta-analysis. Frontiers in Human Neuroscience 2018;12:416. https://doi.org/10.3389/fnhum.2018.00416.
- [22] Andrews SC, Hoy KE, Enticott PG, Daskalakis ZJ, Fitzgerald PB. Improving working memory: the effect of combining cognitive activity and anodal transcranial direct current stimulation to the left dorsolateral prefrontal cortex. Brain Stimulation 2011;4:84–9. https://doi.org/10.1016/j.brs.2010.06.004.
- [23] Windhoff M, Opitz A, Thielscher A. Electric field calculations in brain stimulation based on finite elements: An optimized processing pipeline for the generation and usage of accurate individual head models. Human Brain Mapping 2013. https://doi.org/10.1002/hbm.21479.
- [24] Huang Y, Datta A, Bikson M, Parra LC. Realistic vOlumetric-Approach to Simulate Transcranial Electric Stimulation -- ROAST -- a fully automated open-source pipeline. Journal of Neural Engineering 2019. https://doi.org/10.1088/1741-2552/ab208d.
- [25] Nielsen JD, Madsen KH, Puonti O, Siebner HR, Bauer C, Madsen CG, et al. Automatic skull segmentation from MR images for realistic volume conductor

- models of the head: Assessment of the state-of-the-art. NeuroImage 2018. https://doi.org/10.1016/j.neuroimage.2018.03.001.
- [26] Miranda PC, Mekonnen A, Salvador R, Ruffini G. The electric field in the cortex during transcranial current stimulation. NeuroImage 2013. https://doi.org/10.1016/j.neuroimage.2012.12.034.
- [27] Datta A, Bansal V, Diaz J, Patel J, Reato D, Bikson M. Gyri-precise head model of transcranial direct current stimulation: Improved spatial focality using a ring electrode versus conventional rectangular pad. Brain Stimulation 2009. https://doi.org/10.1016/j.brs.2009.03.005.
- [28] Indahlastari A, Albizu A, O'Shea A, Forbes MA, Nissim NR, Kraft JN, et al. Modeling Transcranial Electrical Stimulation in the Aging Brain. Brain Stimulation 2020;13. https://doi.org/10.1016/j.brs.2020.02.007.
- [29] Antonenko D, Grittner U, Saturnino G, Nierhaus T, Thielscher A, Flöel A. Interindividual and age-dependent variability in simulated electric fields induced by conventional transcranial electrical stimulation. NeuroImage 2021;224:117413. https://doi.org/10.1016/j.neuroimage.2020.117413.
- [30] Indahlastari A, Albizu A, Boutzoukas EM, O'Shea A, Woods AJ. White Matter Hyperintensities Affect Transcranial Electrical Stimulation in the Aging Brain. Brain Stimulation 2020;14:69–73. https://doi.org/10.1016/j.brs.2020.11.009.
- [31] Truong DQ, Magerowski G, Blackburn GL, Bikson M, Alonso-Alonso M. Computational modeling of transcranial direct current stimulation (tDCS) in obesity: Impact of head fat and dose guidelines. NeuroImage: Clinical 2013. https://doi.org/10.1016/j.nicl.2013.05.011.
- [32] Indahlastari A, Albizu A, Kraft JN, O'Shea A, Nissim NR, Dunn AL, et al. Individualized tDCS modeling predicts functional connectivity changes within the working memory network in older adults. Brain Stimulation: Basic, Translational, and Clinical Research in Neuromodulation 2021;14:1205–15. https://doi.org/10.1016/J.BRS.2021.08.003.
- [33] Edwards D, Cortes M, Datta A, Minhas P, Wassermann EM, Bikson M. Physiological and modeling evidence for focal transcranial electrical brain stimulation in humans: A basis for high-definition tDCS. NeuroImage 2013;74:266–75. https://doi.org/10.1016/J.NEUROIMAGE.2013.01.042.
- [34] Suen PJC, Doll S, Batistuzzo MC, Busatto G, Razza LB, Padberg F, et al. Association between tDCS computational modeling and clinical outcomes in depression: data from the ELECT-TDCS trial. European Archives of Psychiatry and Clinical Neuroscience 2020. https://doi.org/10.1007/s00406-020-01127-w.
- [35] Halko MA, Datta A, Plow EB, Scaturro J, Bikson M, Merabet LB. Neuroplastic changes following rehabilitative training correlate with regional electrical field induced with tDCS. NeuroImage 2011;57:885–91. https://doi.org/10.1016/J.NEUROIMAGE.2011.05.026.
- [36] Albizu A, Fang R, Indahlastari A, O'Shea A, Stolte SE, See KB, et al. Machine learning and individual variability in electric field characteristics predict tDCS treatment response. Brain Stimulation 2020. https://doi.org/10.1016/j.brs.2020.10.001.

- [37] Kim S, Yang C, Dong SY, Lee SH. Predictions of tDCS treatment response in PTSD patients using EEG based classification. Frontiers in Psychiatry 2022;13. https://doi.org/10.3389/fpsyt.2022.876036.
- [38] Shinde AB, Mohapatra S, Schlaug G. A machine learning approach to identify the engagement of a brain network targeted by non-invasive brain-stimulation. BioRxiv 2022:2022.09.12.507591. https://doi.org/10.1101/2022.09.12.507591.
- [39] Gullett JM, Albizu A, Fang R, Loewenstein DA, Duara R, Rosselli M, et al. Baseline Neuroimaging Predicts Decline to Dementia From Amnestic Mild Cognitive Impairment. Frontiers in Aging Neuroscience 2021;13:828. https://doi.org/10.3389/FNAGI.2021.758298/BIBTEX.
- [40] Indahlastari A, Albizu A, O'Shea A, Forbes MA, Nissim NR, Kraft JN, et al. Modeling transcranial electrical stimulation in the aging brain. Brain Stimulation 2020. https://doi.org/10.1016/j.brs.2020.02.007.
- [41] Dmochowski JP, Datta A, Huang Y, Richardson JD, Bikson M, Fridriksson J, et al. Targeted transcranial direct current stimulation for rehabilitation after stroke. NeuroImage 2013;75:12–9. https://doi.org/10.1016/j.neuroimage.2013.02.049.
- [42] Khan A, Antonakakis M, Suntrup-Krueger S, Lencer R, Nitsche MA, Paulus W, et al. Can individually targeted and optimized multi-channel tDCS outperform standard bipolar tDCS in stimulating the primary somatosensory cortex? Brain Stimulation 2023;16:1–16. https://doi.org/10.1016/j.brs.2022.12.006.
- [43] Krause MR, Zanos TP, Csorba BA, Pilly PK, Choe J, Phillips ME, et al. Transcranial Direct Current Stimulation Facilitates Associative Learning and Alters Functional Connectivity in the Primate Brain. Current Biology 2017;27:3086-3096.e3. https://doi.org/10.1016/j.cub.2017.09.020.
- [44] Sadleir RJ, Vannorsdall TD, Schretlen DJ, Gordon B. Target optimization in transcranial direct current stimulation. Frontiers in Psychiatry 2012;3:90. https://doi.org/10.3389/FPSYT.2012.00090/BIBTEX.
- [45] Indahlastari A, Albizu A, Nissim NR, Traeger KR, O'Shea A, Woods AJ. Methods to monitor accurate and consistent electrode placements in conventional transcranial electrical stimulation. Brain Stimulation 2019;12:267–74. https://doi.org/10.1016/j.brs.2018.10.016.
- [46] Oostenveld R, Praamstra P. The five percent electrode system for high-resolution EEG and ERP measurements. Clinical Neurophysiology 2001;112:713–9. https://doi.org/10.1016/S1388-2457(00)00527-7.
- [47] Dmochowski JP, Datta A, Bikson M, Su Y, Parra LC. Optimized multi-electrode stimulation increases focality and intensity at target. Journal of Neural Engineering, vol. 8, IOP Publishing; 2011, p. 046011. https://doi.org/10.1088/1741-2560/8/4/046011.
- [48] Chang CC, Lin CJ. LIBSVM: A Library for support vector machines. ACM Transactions on Intelligent Systems and Technology 2011. https://doi.org/10.1145/1961189.1961199.
- [49] Opitz A, Paulus W, Will S, Antunes A, Thielscher A. Determinants of the electric field during transcranial direct current stimulation. NeuroImage 2015. https://doi.org/10.1016/j.neuroimage.2015.01.033.

[50] Laakso I, Tanaka S, Koyama S, De Santis V, Hirata A. Inter-subject variability in electric fields of motor cortical tDCS. Brain Stimulation 2015. https://doi.org/10.1016/j.brs.2015.05.002.